AFRL-RX-WP-TP-2009-4032

AQUEOUS BASED FREEZE-FORM EXTRUSION FABRICATION OF ALUMINA COMPONENTS (PREPRINT)

Tieshu Huang, Michael S. Mason, Xiyue Zhao, Gregory E. Hilmas, and Ming C. Leu

University of Missouri Rolla

JANUARY 2009

Approved for public release; distribution unlimited.

See additional restrictions described on inside pages

STINFO COPY

AIR FORCE RESEARCH LABORATORY
MATERIALS AND MANUFACTURING DIRECTORATE
WRIGHT-PATTERSON AIR FORCE BASE, OH 45433-7750
AIR FORCE MATERIEL COMMAND
UNITED STATES AIR FORCE

REPORT DOCUMENTATION PAGE

Form Approved
OMB No. 0704-0188

1. REPORT DATE *(DD-MM-YY)*	2. REPORT TYPE	3. DATES COVERED *(From - To)*
January 2009	Journal Article Preprint	01 January 2009 – 31 January 2009

4. TITLE AND SUBTITLE
AQUEOUS BASED FREEZE-FORM EXTRUSION FABRICATION OF ALUMINA COMPONENTS (PREPRINT)

5a. CONTRACT NUMBER
FA8650-04-C-5704

5b. GRANT NUMBER

5c. PROGRAM ELEMENT NUMBER
78011F

6. AUTHOR(S)
Tieshu Huang, Michael S. Mason, Xiyue Zhao, Gregory E. Hilmas, and Ming C. Leu

5d. PROJECT NUMBER
2865

5e. TASK NUMBER
25

5f. WORK UNIT NUMBER
25100000

7. PERFORMING ORGANIZATION NAME(S) AND ADDRESS(ES)
University of Missouri at Rolla
Department of Materials Science and Engineering
1870 Miner Circle
Rolla, MO 65409-0970

8. PERFORMING ORGANIZATION REPORT NUMBER
AFRL-RX-WP-TP-2009-4032

9. SPONSORING/MONITORING AGENCY NAME(S) AND ADDRESS(ES)
Air Force Research Laboratory
Materials and Manufacturing Directorate
Wright-Patterson Air Force Base, OH 45433-7750
Air Force Materiel Command
United States Air Force

10. SPONSORING/MONITORING AGENCY ACRONYM(S)
AFRL/RXLMP

11. SPONSORING/MONITORING AGENCY REPORT NUMBER(S)
AFRL-RX-WP-TP-2009-4032

12. DISTRIBUTION/AVAILABILITY STATEMENT
Approved for public release; distribution unlimited.

13. SUPPLEMENTARY NOTES
This work was funded in whole or in part by Department of the Air Force contract FA8650-04-C-5704. The U.S. Government has for itself and others acting on its behalf an unlimited, paid-up, nonexclusive, irrevocable worldwide license to use, modify, reproduce, release, perform, display, or disclose the work by or on behalf of the U.S. Government. Technical paper contains color.

PAO Case Number and clearance date: 88ABW-2008-1140, 26 November 2008

14. ABSTRACT
Fabricating ceramic materials into complex 3-D components is typically a complicated, costly, and time-consuming process that involves diamond machining to achieve its final shape. In most cases, the initial processing is powder-based, followed by densification (sintering) at elevated temperatures. Only a few circumstances, such as fuse casting and thermal spraying, can ceramics be directly fabricated into near net-shape, fully dense ceramic components. However, these techniques require an extremely high temperature to melt the ceramic.

15. SUBJECT TERMS
solid freeform fabrication, freeze-form, extrusion, alumina, aqueous, ceramic, paste

16. SECURITY CLASSIFICATION OF: a. REPORT	b. ABSTRACT	c. THIS PAGE	17. LIMITATION OF ABSTRACT:	18. NUMBER OF PAGES	19a. NAME OF RESPONSIBLE PERSON (Monitor)
Unclassified	Unclassified	Unclassified	SAR	30	Todd J. Turner
					19b. TELEPHONE NUMBER *(Include Area Code)* N/A

Standard Form 298 (Rev. 8-98)
Prescribed by ANSI Std. Z39-18

Aqueous Based Freeze-form Extrusion Fabrication of Alumina Components

Tieshu Huang, Michael S. Mason, Xiyue Zhao, Gregory E. Hilmas, and Ming C. Leu

Research Paper

Purpose

The purpose of this research is to develop an inexpensive and environmentally friendly solid freeform fabrication technique, called the Freeze-form Extrusion Fabrication (FEF), and use this technique in advanced ceramic fabrication.

Design/methodology/approach

FEF uses a highly loaded aqueous ceramic paste (≥50 vol.% solids loading) with a small quantity (~2 vol.%) of organic binder to fabricate a ceramic green part layer by layer with a computer controlled 3-D gantry machine at a temperature below the freezing point of the paste. Further, a freeze-drying technique is used for preventing deformation and the formation of cracks during the green part drying process. Following the freeze-drying, the ceramic green part undergoes binder removal and is sintered to near full density.

Findings

Extrudable, alumina pastes of high solids loading and process parameters for FEF processing of these pastes have been developed. Paste rheological properties and stability, extrusion rate, 3-D gantry motion speed and other process parameters strongly affect the quality of the final ceramic parts. The minimum deposition angle, which reflects the maximum amount of extrusion offset to produce components with overhanging features without using support materials, is strongly related to the fabrication (environment) temperature. The lower the fabrication temperature, the lower the minimum deposition angle that could be achieved. Four

point bending flexure strengths of the FEF processed Al_2O_3 test samples were 219 MPa and 198 MPa for longitudinally deposited and transversely deposited samples, respectively. Major defects, which limited the strength of the materials, were due to under filling during the extrusion.

Practical implications

Successful development of the FEF technique will introduce a new approach to manufacturing ceramic materials into useful, complex shapes and components. The significant advantages of this technique include the use of environmentally friendly processing medium (water), inexpensive method of medium removal (freeze-drying), and a much smaller quantity of organic binder to remove by pyrolysis techniques. The products can be sintered to near full density.

Keywords: Solid Freeform Fabrication, Freeze-form, Extrusion, Alumina, Aqueous, Ceramic, Paste.

I. Introduction

Fabricating ceramic materials into complex 3-D components is typically a complicated, costly, and time-consuming process that involves diamond machining to achieve its final shape. In most cases, the initial processing is powder-based, followed by densification (sintering) at elevated temperatures. Only in a few circumstances, such as fuse casting and thermal spraying, can ceramics be directly fabricated into near net-shape, fully dense ceramic components. However, these techniques require an extremely high temperature to melt the ceramic. More commonly, 3-D ceramic components are produced by casting the materials into a prefabricated mold, designed to mimic the shape of the final product, and once again sintered to achieve near full density. The costs and manufacturing time associated with mold design and processing increases significantly with complexity of the component. Furthermore, many 3-D components cannot be produced by a mold-based fabrication process, such as components with internal passages or cavities.

In recent years, quite a few solid freeform fabrication (SFF) techniques have been developed and used to fabricate complex, 3-D ceramic components. They include the following: Fused Deposition of Ceramics (FDC) [Rangarajan, et al., 2000, Lous, et al., 2000, Bandyopadhyay, et al., 2000, Bellini, 2002, and Danforth, et al., 1998], Fused Deposition Modeling (FDM) [Crump, 1992], Extrusion Freeform Fabrication (EFF) [Hilmas, et al., 1996 and Wang, et al., 2004], slurry and binder-based 3-D Printing (3DP) [Cima, et al., 2001], Chemical Liquid Deposition (CLD) [He and Zhou, 2000], Selective Laser Sintering (SLS) [Beaman et al. 1997 and Kruth, et al., 2004], Selective Laser Melting (SLM) [Kruth, et al., 2004 and Klocke and Ader, 2003], Shape Deposition Manufacturing (SDM) [Cooper, et al., 2002 and Stampfl, et al., 2001], Robocasting [Cesarano, et al., 1998, 1999 and He, et al., 2000, 2001] and

Laser Engineered Net Shaping (LENS) [Balla, et al., 2008]. All of these techniques are layer-by-layer addition techniques. Some of them are direct fabrication techniques, while others are indirect. Some of these techniques can achieve high final density in ceramic components, such as EFF, FDC, CLD, SDM, SLS, and Robocasting, because of the high green density and a separate sintering process. Some of the techniques can achieve smooth surface finish (typical surface roughness between 200 and 500 μm), including Slurry-3DP, CLD, SLS, SLM, SDM, and Robocasting. Most of them are organic binder or solvent based, and are thus not friendly to the environment. However, the SLM and SDM techniques are considered to be environmental friendly.

Extrusion related solid freeform fabrication techniques, such as EFF, FDC, and Robocasting, are among the most developed SFF techniques. EFF was the first technique to utilize extrusion of slurries (organic based) and to produce 3-D, functionally graded materials (FGMs) such as ceramic oxides graded to inconel or stainless steel [Hilmas, et al., 1996]. Robocasting (aqueous based extrusion) has been used to produce parts from different types of ceramics including oxides and non-oxides, biomaterials, and FGMs such as Si_3N_4 graded to W [Cesarano, et al., 1998, 1999, He, et al., 2000, 2001, and Lewis, et al., 2006]. Aqueous based SFF has several unique advantages: (1) it is environmentally friendly; (2) minimal binder content reduces time for binder pyrolysis; (3) the equipment cost is low compared with laser based processes such as selective laser sintering; and (4) the process can accommodate multiple materials to make functionally graded components.

Freeze-form Extrusion Fabrication (FEF) is a layer-by-layer extrusion manufacturing process developed by extending the concept of Rapid Freeze Prototyping (RFP) [Sui and Leu, 2003a, 2003b, Bryant, et al., 2003, Leu, et al., 2003, and Liu and Leu, 2007]. An aqueous paste

in the FEF process is extruded through a nozzle, which moves in a plane, using a ram extruder, and the extruded material immediately deposits on a working surface. The whole fabrication gantry system is set to a temperature designed to freeze the paste as it is deposited. Due to the environment temperature being lower than the paste freezing temperature, the extruded material freezes quickly to form solid. After one layer is finished, the z-axis moves up a distance that is equal to the layer thickness. The nozzle follows a contour that is generated by a computer according to a given CAD model. The computer slices a complex 3-D shape into 2-D slices. The thickness of each slice is the same as the thickness of each fabrication layer. The stacked 2-D slices form the 3-D part. FEF has some unique advantages, including the ability to fabricate parts directly from pastes, as well as high sintered density and environmental friendliness. It differs from robocasting in that the fabrication process is performed below the paste freezing temperature. Due to the low-temperature environment the extruded paste freezes immediately during the layered deposition. This allows parts of larger size to be made relative to fabrication of green parts from aqueous pastes at room temperature.

This paper discusses the development of the FEF process for use in fabricating 3-D ceramic components. The developed fabrication equipment and process, as well of the post-fabrication processes including freeze-drying, binder burnout and sintering, are described. The temperature effect on the deposition offset has been studied using the “minimum deposition angle” test. The mechanical properties and microstructures of FEF fabricated samples are also presented. The ceramic used in this study is aluminum oxide (Al_2O_3), one of the most common high-temperature structural ceramic materials. Al_2O_3 is lightweight and inexpensive. Further, it exhibits high strength and hardness to elevated temperatures (>1500 °C) in an oxidizing atmosphere, making it one of the most important refractory ceramic insulator materials.

II. Experimental Procedures

The raw materials used in this study included Al_2O_3 powder (A-16SG, 0.4 µm particle size, Mineral and Pigment Solutions, Inc., South Plainfield, NJ), a binder (Aquazol 50, 5000 MW, ISP Technologies, Inc., Wayne, NJ), and a lubricant or plasticizer (Polyethylene glycol, PEG-400, Aldrich, St. Louis, MO). The manufacturer of Al_2O_3 powder added 500 ppm MgO as a sintering aid. Glycerol (Aldrich, St. Louis, MO) was added to the material mixture to assist in avoiding the formation of large, elongated ice crystals during the freezing process. Darvan C (R. T. Vanderbilt, Norwalk, CT) was used as a dispersant to assist in achieving uniform mixing. Distilled water was used as the medium, and a 5-8% HCl water solution was used to adjust the pH value as needed.

Figure 1 shows a flowchart of the paste preparation process. The solids loading used for the current study was 50 vol.% Al_2O_3. The dispersant content was 1 - 2 wt.% of the weight of the ceramic solids. The binder content was 2 vol.%. A vacuum mixer (Whip Mix, Model F, Louisville, KY) was used for degassing and adjustment of paste rheological properties. 6 vol.% of glycerol was added to optimize water crystallization. PEG-400 was added to a content of 1 vol.% as lubricant. Finally, the paste's viscosity was adjusted by changing the pH value of the paste from a range of 12 - 14 to a range of 8.5 - 9.5. A viscosity check was the final step to ensure the paste's desirable extrusion behavior. To prevent evaporation of water in the paste, the batched paste was collected immediately after vacuum mixing and sealed in 60 cm^3 plastic syringes.

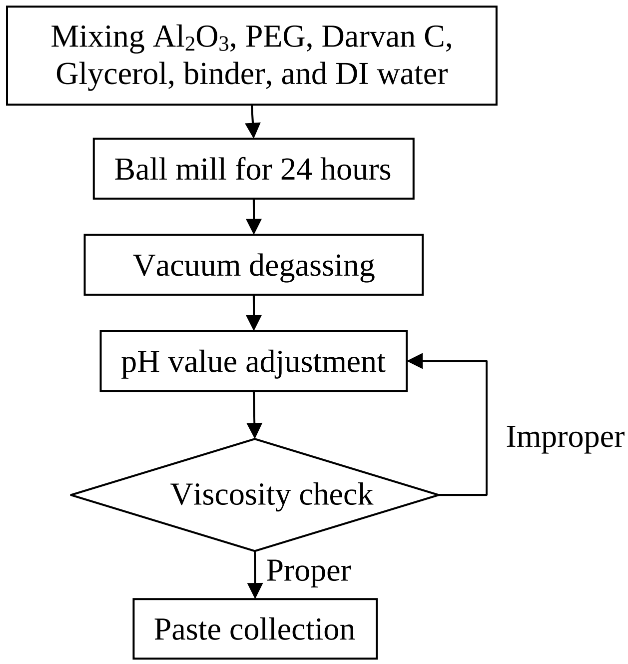

Figure 1. Flowchart for the paste preparation process.

All mechanical test samples, and other ceramic components produced in this study, were fabricated on a computer-controlled 3-D gantry system (Figure 2). The 3-D gantry system consisted of three orthogonal linear axes (X, Y, Z) from Velmex BiSlide (Velmex, Bloomfield, NY), each with a 300 mm travel range. DC motors (Pacific Scientific PMA22B), each with a resolver for position feedback at a resolution of 1000 counts per revolution were used for driving the axes. Each motion axis had a maximum speed of 127 mm/s and a resolution of 2.54 µm. All the axes were controlled by a Delta-Tau Turbo PMAC PCI board. The 3-D gantry was set up inside a freezer with a temperature range from 0 to –30 °C as needed. Heating coils were installed around the extruder and the nozzle areas to keep the paste from freezing.

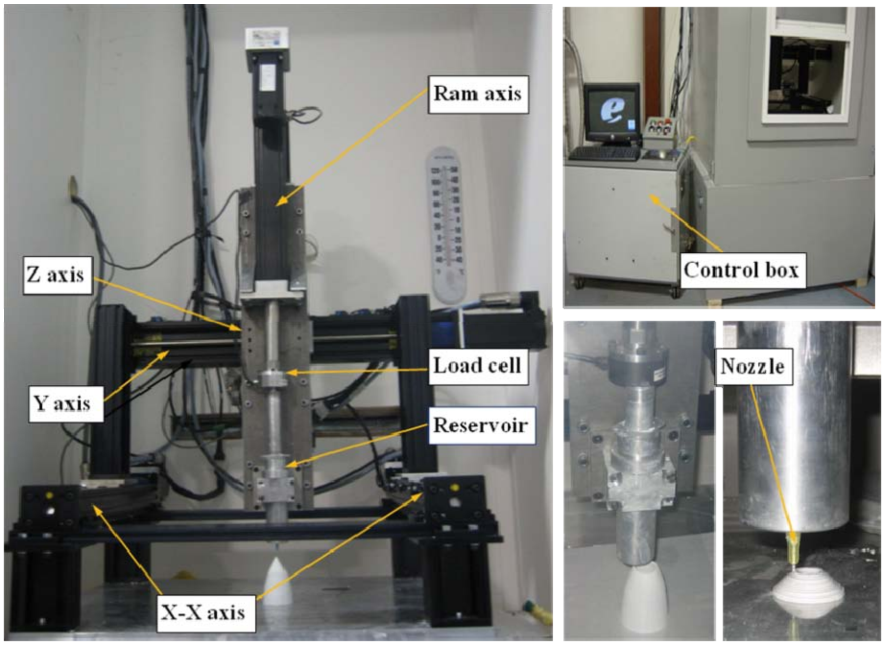

Figure 2. FEF 3-D extrusion-deposition gantry system.

After FEF processing, the main binder (frozen water) was removed from the Al_2O_3 samples through sublimation by using a freeze dryer (Virits, Model Genesis 25, Gardiner, NY) programmed to a schedule of time-temperature-pressure (Figure 3), which depends on the dimensions of the sample. After freeze drying, the samples were pyrolyzed to remove the remaining organics using a 0.5 °C/min ramp-up to 600 °C and holding for two hours, followed by cooling at 10 °C/min to room temperature. The samples were then sintered at 1550 °C for two hours using a heating rate of 5 °C/min and a cooling rate of 10 °C/min. The density of the sintered samples was measured using Archimedes method. Research on the relationship between rheological property and binder content was performed using different batches, which have the binder content varied from 1 to 5 vol.% with 1 vol.% resolution. Testing the effect of binder content on paste viscosity was performed on batches containing 2 vol.% dispersant. The dispersant, Darvan C, was used to disperse the Al_2O_3 particles in the paste formulation. The

dispersion effect depends mostly on the dispersant content and the system's pH value. As a neutral binder, Aquazol 50 does not change the paste pH value significantly, so the effect of the dispersant content was tested prior to binder addition.

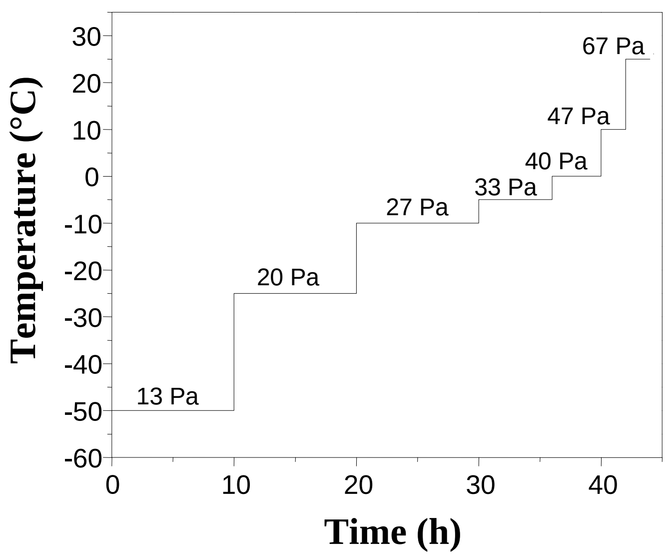

Figure 3. Freeze drying temperature-time-pressure schedule.

The minimum deposition angle, which is the minimum angle that can be achieved between the substrate and the slope of a hollow cone without collapse, depends primarily on the paste properties and environment temperature. This angle reflects the offset ability of the FEF process in fabricating a 3-D part with overhanging without using a support material. The tested temperatures included 20 °C, 10 °C, 0 °C, -10 °C, and -20 °C. In each set of tests, hollow cones were fabricated using bottom diameters of 38 mm, 51 mm, and 64 mm. For calculation of the minimum deposition angle, the cone height was varied to determine the lowest height without collapse of the cone during the building process. Figure 4 is a schematic drawing that shows the minimum deposition angle, α, and other parameters.

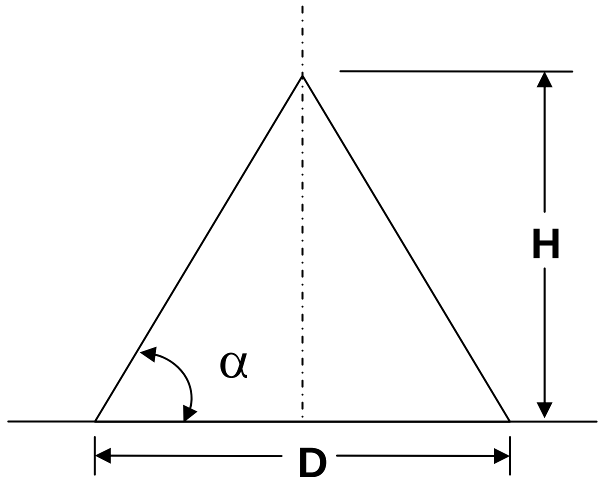

Figure 4. The minimum deposition angle α.

Mechanical property test samples were fabricated using the FEF process in two architectures at -20 °C using the same fabrication parameters. The parameters are 580 μm nozzle diameter, 20 mm/s nozzle moving speed, 500 μm layer thickness, and 40 kg extrusion force. The first architecture had deposition of paste along the longitudinal direction of the sample (termed hereafter LD), while the second architecture had deposition along the transverse direction of the sample (termed hereafter as TD). The fabricated samples were then processed by diamond machining to ASTM C-1161 standard "B" bars, which had the nominal dimensions of 45 mm × 4 mm × 3 mm. A total of 40 samples (26 LD and 14 TD samples) were fabricated for mechanical testing. Four point bending tests were performed on a screw-driven mechanical test frame (Instron, Model 5881, Norwood, MA). Fracture surfaces of tested samples were examined by scanning electron microscopy (SEM) techniques (Jeol 330, Peabody, MA). Various 3-D shapes were fabricated to demonstrate the feasibility of FEF.

III. Results and Discussion

3.1. Rheological properties of paste

The test results of paste rheological property (Figure 5) showed that the viscosity decreased as the dispersant concentration increased when the dispersant content was less than 1.5 vol.%. However, the viscosity increased with dispersant content when the dispersant was greater than 1.5 vol.%, due to double layer compression. The results also showed that the pastes exhibited a shear thinning behavior for all ranges of dispersant content. The viscosity was found to increase with the binder content (Figure 6) as expected. Binder additions of 2-4 vol.% were adopted in the paste preparation because these pastes exhibited a low enough viscosity (~ 50 Pa·s) in the high shear rate range to be extrudable at low pressures, while having a high enough viscosity (~ 200 Pa·s) in the low shear rate range to quickly become rigid and provide green strength after extrusion and prior to becoming frozen. The paste viscosity was controllable through adjustment of pH value by adding 0.5 - 0.8 vol.% of a 5 - 8% HCl acid water solution.

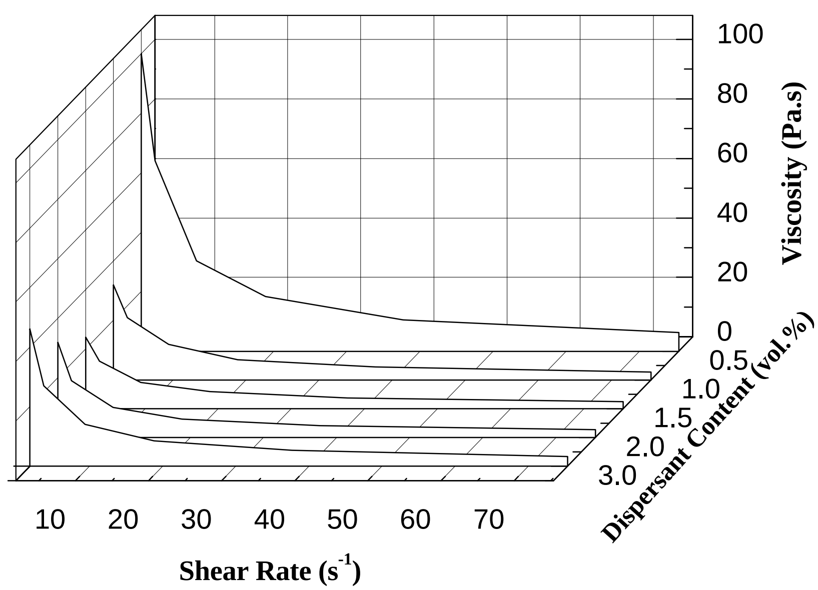

Figure 5. Viscosity as a function of shear rate and dispersant content.

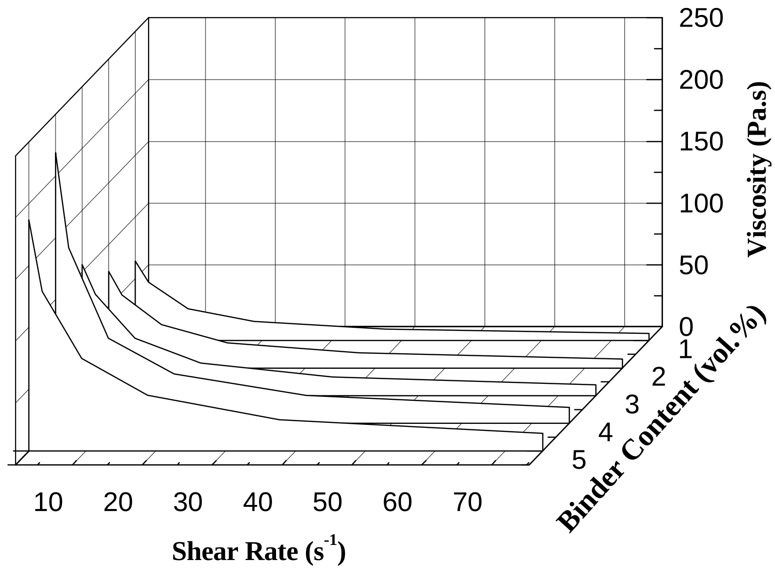

Figure 6. Viscosity as a function of shear rate and binder content.

3.2. Layer thickness, extrusion rate, and deposition speed

For a desirable deposition in the extrusion deposition process, layer thickness, extrusion rate, and deposition speed need to be properly coordinated and controlled. The desirable combination is the combination that can be used to build parts without overfilling and/or underfilling defects, and to achieve uniform and dense microstructures after all of the processing steps are complete. Trial and error is an empirical approach to arrive at appropriate parameter combinations. However, it requires a considerable number of experiments to achieve proper values of processing parameters. A theoretical guide is needed in selecting the values of these parameters.

The first parameter to be determined is the deposition speed since it is strongly related to the fabrication efficiency. The deposition speed is desired to be as high as possible. However, the deposition speed of the FEF technique is limited due to the freezing rate and it is related to the extrusion rate. The layer thickness is the second parameter. Layer thickness is related to the

extrusion rate and deposition speed. It influences how the currently deposited material is attached and adhered to the previously deposited material. The ideal shape of the extrudate should be a slab (which is flat on the top and bottom sides) rather than a round cross section. A slab shape has the advantage of being able to provide increased adhesion between the currently deposited material and the material in the previously deposited layers. The second advantage of the slab shape is the reduced amount of material migration that is required to fill the gaps between the extruded filaments. A slab-shaped cross section can be achieved by flattening the extruded material with the nozzle tip as the material is being extruded.

Figure 7 consists of schematic drawings showing the dimensions of the nozzle, extrudate, and extrusion parameters. Equations (1) and (2) represent the relationship between the various variables under the ideal conditions to form a slab shape of extrudate. The ideal conditions are: First, the nozzle standoff distance is smaller than the diameter of the extrudate after leaving the nozzle; Second, the paste is thick enough to keep its shape after extrusion when no outside force is applied.

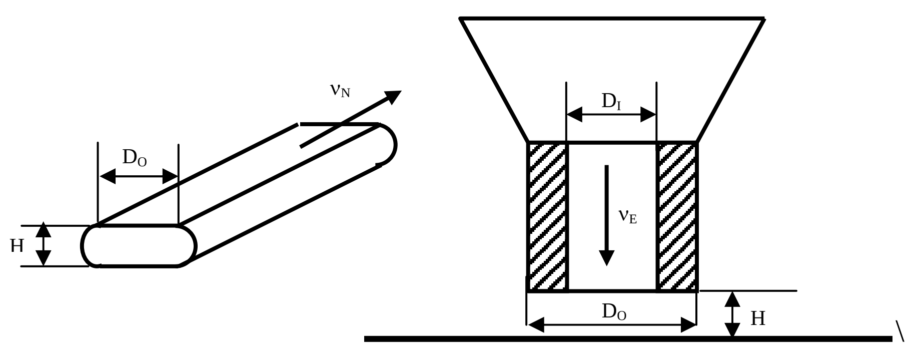

Figure 7. Schematic drawings showing the dimensions of the nozzle and slab shaped extrudate.

$$v_N = v_E \frac{\pi D_I^2}{4HD_O + \pi H^2} = v_E K \quad (1)$$

$$K = \frac{\pi D_I^2}{4HD_O + \pi H^2} \quad (2)$$

where:

v_N: Nozzle moving speed (i.e. paste deposition speed)

v_E: Extrusion speed (i.e., paste flowing speed inside the nozzle)

D_I: Inside diameter of the nozzle

D_O: Outside diameter of the nozzle

H: Nozzle standoff distance

The extrusion speed is related to the rheological properties of paste, which are affected by solids loading, particle surface chemistry, dispersing condition, liquid phase migration, etc. If the paste's rheological properties are consistent, the extrusion speed v_E can be set to and maintained at a desired value by closed-loop feedback control. This is another aspect of our FEF research. Some results of our feedback control research for this process can be found in [Mason et al., 2008 and Zhao et al., 2008].

3.3. Temperature effect on minimum deposition angle

A completed cone with 19 mm height and 38.1 mm bottom diameter and a collapsed cone are shown in Figure 9. The minimum deposition angles were obtained from the successfully fabricated cones with the minimum height for each bottom diameter. Three sets of tests were conducted to fabricate cones with different bottom diameters to find the relationship between the minimum depositioin angle and the environment temperature.

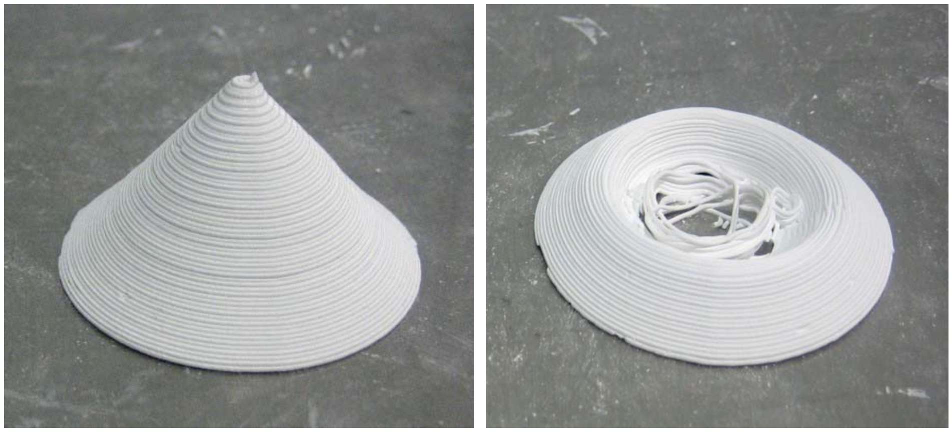

Figure 9. A completed cone vs. a collapsed cone.

The results obtained on the minimum deposition angles are shown in Figure 10. It can be seen that the minimum deposition angle decreased markedly as the environment temperature was decreased and this effect became more pronounced when the temperature was below 0 °C. This is because the paste viscosity increased as the environment temperature decreased, and when the temperature reached below the paste freezing temperature the extruded paste became frozen in a short time. The minimum deposition angle increased as the cone diameter increased when the temperature was above -10 °C. This is expected because there is more weight from newly deposited paste that needs to be supported by previously deposited paste in the bottom when the cone diameter is larger. The minimum deposition angle decreased as the cone diameter increased when the temperature was below -10 °C. This phenomenon was more significant at lower temperatures. A possible reason was that a larger cone needed a longer time to complete each layer, allowing more time for the deposited paste to freeze. This provided a stronger support for the deposition of future layers.

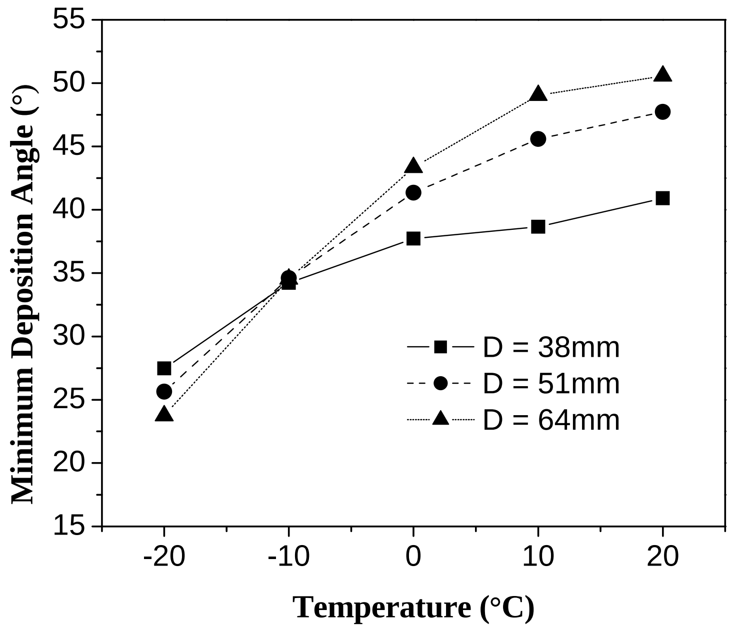

Figure 10. Minimum deposition angle as a function of temperature for three sample sizes.

3.4. Mechanical properties and microstructures

The average flexural strength of the LD samples was 219 MPa, and the minimum and maximum strengths of these samples were 150 and 327 MPa, respectively. The average flexural strength of the TD samples was 198 MPa, and their minimum and maximum strengths were 168 and 228 MPa, respectively. The typical flexural strength of dense alumina from relevant literature is 300 - 500 MPa [Boch and Niepce, 2007]. The tested values from our samples were lower than the referenced values mainly due to underfilling, which results in porosity and markedly affects strength. The Weibull plot of the LD samples is shown in Figure 11. For the LD samples the Weibull Modulus is m=5.44. This value is relatively low, thus further research will be needed to optimize the process parameters for minimizing defects.

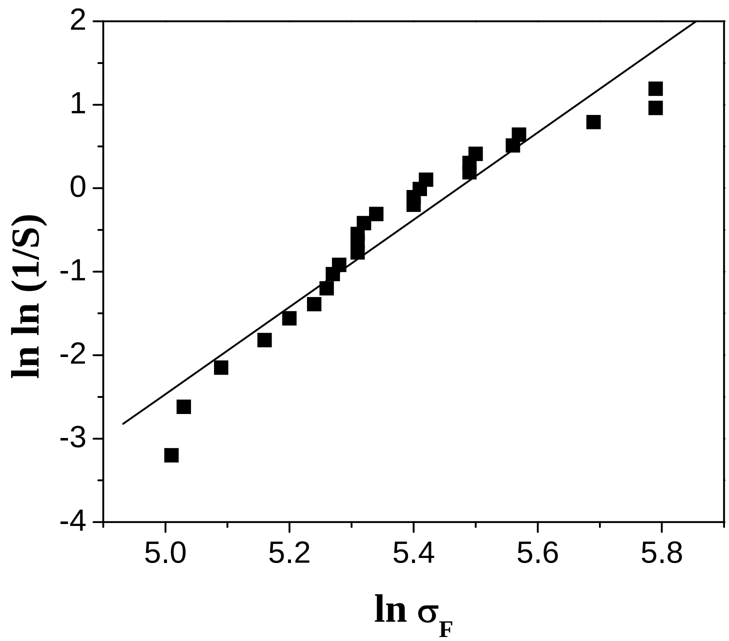

Figure 11. Weibull plot for the LD samples.

The fracture surfaces of test samples were analyzed using scanning electron microscopy (SEM). The LD samples exhibited a more uniform microstructure than the TD samples. The left image of Figure 12 shows a clear gap due to underfilling between the deposited threads. The right image of Figure 12 shows a SEM image of a typical fracture surface from an LD sample. The image shows that the sample exhibited a pattern of brittle fracture, with the crack cleaving the majority of the grains in a transgranular fashion. Most of the LD samples exhibited a relatively dense microstructure compared with the TD samples, with only a few samples showing some small pores distributed throughout the fracture surface. A few LD samples contained large pores on the fracture surface, presumably as a result of underfilling during the FEF processing. The TD samples clearly showed that underfilling was a major problem for this deposition architecture.

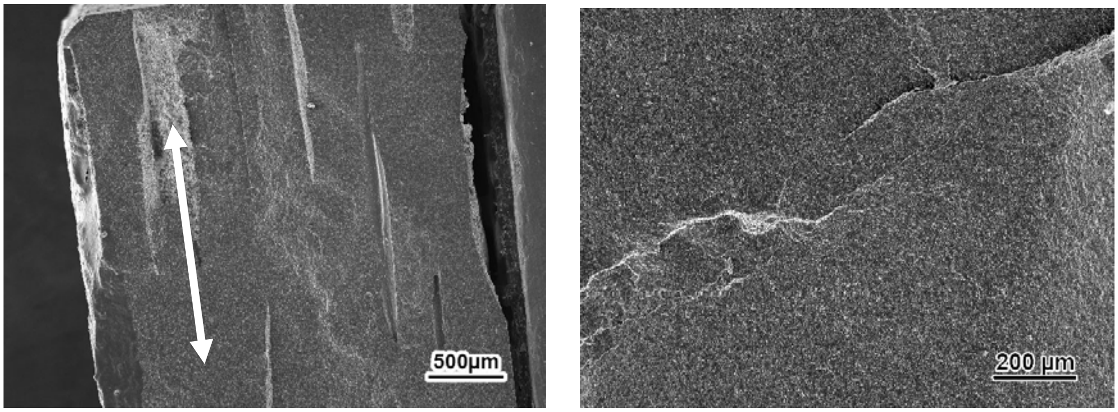

Figure 12. SEM micrographs showing the fracture surfaces of typical alumina test bars fabricated by the FEF process. Left: a fracture surface of a TD sample that contains a gap due to underfilling. The arrow shows the deposition direction. Right: a typical LD sample fracture surface with a uniform microstructure exhibiting brittle fracture.

3.5. Feasibility of FEF process

To demonstrate the feasibility of fabrication of Al_2O_3 components using the FEF process, tangent ogive hollow cones were fabricated. Figure 15 shows a photo of the sintered Al_2O_3 cones fabricated using a 580 µm diameter extrusion nozzle. The cones were fabricated at -20 °C and then freeze-dried in a freeze dryer. The green cones had approximately 50 % of its theoretical density. The surface roughness of green parts was approximately 100 – 200 µm. After sintering, the cones achieved approximately 98% of the theoretical density.

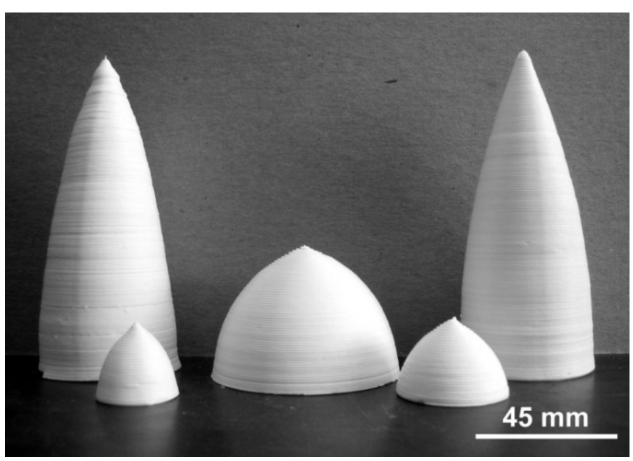

Figure 14. Optical Image showing Al_2O_3 tangent ogive hollow cones fabricated using FEF technique at -20 °C.

IV. Conclusions

An environmentally friendly solid freeform fabrication process called the Freeze-form Extrusion Fabrication (FEF) has been developed to produce ceramic components by extruding, depositing, and freezing aqueous ceramic pastes layer by layer. This study has demonstrated successful fabrication of ceramic components with this novel solid freeform fabrication technique. The developed FEF system was described and the major process parameters were discussed. Aqueous pastes consisting of a 50 vol.% solids loading of Al_2O_3 ceramic powder with a small amount of organic binder content showed favorable extrusion behavior. The dispersant, binder content, and pH value strongly affected the paste rheological properties and governed the paste extrusion behavior. The ability of the FEF process to build overhanging features without the use of support material was verified through minimum deposition angle tests. Environment temperature significantly affected the minimum deposition angle. The average flexure strengths of FEF processed, sintered Al_2O_3 samples were 219 MPa and 198 MPa for longitudinally and transversely deposited samples, respectively. The FEF samples possess uniform microstructures with some large deposition defects because of underfilling. The longitudinally deposited samples had considerably fewer defects than the transversely deposited samples.

Acknowledgement

This work was supported by the Air Force Research Laboratory under Contract FA8650-04-C-5704.

References

Balla, V. K., Bose, S., and Bandyopadhyay, A., (2008) "Processing of Bulk Alumina Ceramics Using Laser Engineered Net Shaping," *International Journal of Applied Ceramic Technology*, doi:10.111/j.1744-7402.2008.02202.x (online early article)

Bandyopadhyay, A., Panda, P. K., Agarwala, M. K., Danforth, S. C., and Safari, A., (2000) "Processing of Piezocomposites by Fused Deposition Technique," *Journal of American Ceramic Society*, Vol. 80, No.6, pp. 1366-72.

Bellini, A, (2002) "Fused Deposition of Ceramics: A comprehensive Experimental, Analytical and Computational Study of Material Behavior, Fabrication Process and Equipment Design," *Ph.D. Dissertation*, Drexel University, Department of Mechanical Engineering, Philadelphia Pennsylvania.

Boch, P. and Niepce, J-C., (2007) "Ceramic Materials: Processes, Properties and Applications," ISTE USA, Newport Beach, CA, USA, pp. 205.

Bryant, F., Sui, G., and Leu, M. C., (2003) "A Study on the Effects of Process Parameters in Rapid Freeze Prototyping," *Solid freeform Journal*, Vol. 9, No. 1, pp. 19-23.

Beaman, J. J., Barlow, J. W., Bourell, D. L., Crawford, R. H., Marcus, H. L., and McAlea, K. P., (1997) *Solid Freeform Fabrication: A New Direction in Manufacturing*, Kluwer Academic Publisher, Norwell, MA, pp. 25-49.

Cesarano, J. III, (1999) "A review of robocasting technology," *Solid Freeform and Additive Fabrication: a Materials Research Society Symposium*; Boston, MA, pp.133-139

Cesarano, J. III, Segalmen, R. and Calvert, P., (1998) "Robocasting Provides Moldless Fabrication from Slurry Deposition," *Ceram. Ind.*, Vol.148, pp. 94-102

Cima, M.J., Oliveira, M., Wang, H.R., Sachs, E., and Holman, R., (2001) “Slurry-Based 3DP and Fine Ceramic Components,” *Proceedings of Solid Freeform Fabrication Symposium*, Austin, Texas, pp. 216-223.

Cooper, Alexander G., Kietzmen, John W., Prinz, Friedrich B., (2002) “Mold Shape Deposition Manufacturing,” U.S. Patent, No. US6375880 B1.

Crump, S. S., (1992) “Appartus and Method for Ceramic Three-Dimensioal Objects” U.S. Patent No. US 5121329.

Danforth, S. C., Agarwala, M., Bandyopadghyay, A., Langrana, N., Jamalabad, V. R., Safari, A. and Van Weeren, R., (1998) “Solid Freeform Fabrication Methods,” U.S. Patent No. US 5738817.

He, G., Hirschfeld, D. A., Cesarano, J. III, Stuecker, J. N., (2001) “Robocasting and Cofiring of Functionally Graded Si_3N_4–W Materials,” *Ceramic Engineering and Science Proceeding*, Vol. 22 pp. 119-125.

He, G., Hirschfeld, D. A., Cesarano, J., III, Stuecker, J. N., (2000) “Processing of Silicon Nitride-Tungsten Prototypes.” *Ceramic Transactions* Vol. 114, pp. 325-332.

He, Z., and Zhou, J. G., (2000) “Feasibility Study of Chemical Liquid Deposition Based Solid Freeform Fabrication,” *Journal of Materials and Design,* Vol. 21, pp.83-92.

Hilmas, G. E., Lombardi, J. L., and Hoffman, R. A., (1996) “Advances in the Fabrication of Functional Graded Materials using Extrusion Freeform Fabrication,” *Functionally Graded Materials,* pp. 319-324 .

Klocke, F, and Ader, C., (2003) “Direct Laser Sintering of Ceramics,” *Proceedings of Solid Freeform Fabrication Symposium*, Austin, Texas, pp. 447-455.

Kruth,, J. P., Mercelis1, P., Froyen2, L., and Rombouts, M., (2004) “Binding Mechanisms in Selective Laser Sintering and Selective Laser Melting,” *Proceedings of Solid Freeform Fabrication Symposium*, Austin, Texas, pp. 44-59.

Leu, M. C., Zhang, W., and Sui, G., (2000) “An Experimental and Analytical Study of Ice Part Fabrication with Rapid Freeze Prototyping,” *Annals of the CIRP*, Vol. 49/1, pp. 147-150.

Liu, Q., and Leu, M. C., (2007) “Finite Element Analysis of Solidification in Rapid Freeze Prototyping,” *ASME Journal of Manufacturing Science and Engineering*, Vol. 129, No. 4, pp. 810-820.

Lewis, J. A., Smay, J. E., Stuecker, J., and Cesarano, J. III., (2006) “Direct Ink Wrinting of Three-Dimensional Ceramic Structures,” *Journal of American Ceramic Society*, Vol. 89 No.12, pp. 3599-3609.

Lous, G. M., Cornejo, I. A., McNlty, T. F., and Danforth, S. C., (2000) “Fabrication of Piezoelectric Ceramic/Polymer Composite Transducers Using Fused Deposition of Ceramics,” *Journal of American Ceramic Society,* Vol. 83, No.1, pp. 124-28.

Mason, M. S., Huang, T. S., Landers, R. G., Leu, M. C., and Hilmas, G. E., (2008) “Aqueous-based Extrusion of High Solids Loading Ceramic Pastes: Process Modeling and Control,” *Proceedings of 2008 International Symposium on Flexible Automation*, Atlanta, Georgia.

Rangarajan, S., Qi, G., Venkataramen, N., Safari, A., and Danforth, S. C., (2000), “Powder Processing, Rheology, and Mechanical Properties of Feedstock for Fused Deposition of Si_3N_4 Ceramics,” *Journal of American Ceramic Society,* Vol. 83, No.7, pp. 1663-69.

Stampfl, J., Cooper, A., Leitgeb, R., Cheng, Y., Prinz, F., (2001) "Shape Deposition Manufacturing of Microscopic Ceramic and Metallic Parts Using Silicon Molds," U.S. Patent, No. US 6242163 B1

Sui, G., and Leu M. C., (2003) "Investigation of Layer Thickness and Surface Roughness in Rapid Freeze Prototyping," *ASME Journal of Manufacturing Science and Engineering*, Vol. 125, No. 3, pp. 556-563.

Sui, G., and Leu M. C., (2003) "Thermal Analysis of Ice Wall Built by Rapid Freeze Prototyping," *ASME Journal of Manufacturing Science and Engineering*, Vol. 125, No. 4, pp. 824-834.

Wang, J. W., Shaw, L. L., Xu, A., and Cameron, T. B., (2004) "Solid Freeform Fabrication of Artificial Human Teeth," *Proceedings of Freeform Fabrication Symposium*, Austin, Texas, pp. 816-825.

Zhao, X., Landers, R. G., and Leu, M. C., (2008) "Adaptive Control of Freeze-form Extrusion Fabrication Process," *Proceedings of 2008 ASME Dynamic Systems and Control Conference*, Ann Arbor, Michigan.